

Reorganization energy of electron transfer at the solvent glass transition

Pradip K. Ghorai and Dmitry V. Matyushov*

*Department of Chemistry and Biochemistry and the Center for the Early Events in Photosynthesis,
Arizona State University, PO Box 871604, Tempe, AZ 85287-1604*

(Dated: June 24, 2018)

We present a molecular-dynamics study of the solvent reorganization energy of electron transfer in supercooled water. We observe a sharp decrease of the reorganization energy at a temperature identified as the temperature of structural arrest due to cage effect as discussed by the mode coupling theory. Both the heat capacity and dielectric susceptibility of the pure water show sharp drops at about the same temperature. This temperature also marks the onset of the enhancement of translational diffusion relative to rotational relaxation signaling the break-down of the Stokes-Einstein relation. The change in the reorganization energy at the transition temperature reflects the dynamical arrest of the slow, collective relaxation of the solvent related to Debye relaxation of the solvent dipolar polarization.

I. INTRODUCTION

Theories of activated chemical dynamics and transport phenomena in condensed phase are often based on transition-state ideas invoking equilibrium thermodynamics to describe the reaction flux across the transition-state surface separating the reactants from the products. The Marcus-Hush theory of electron transfer (ET) reactions fully relies on the transition-state formalism defining the ET activation barrier in terms of two thermodynamic parameters, the free energy gap and the nuclear reorganization energy. The former is the difference in free energies between the final and initial ET states, and the latter determines the curvature of two free energy parabolas.¹ When the donor-acceptor energy gap ΔE is chosen as the reaction coordinate, the classical reorganization energy is given through the energy gap second cumulant:

$$\lambda_s = \langle (\delta\Delta E)^2 \rangle / 2k_B T. \quad (1)$$

The transition-state description becomes inapplicable when the time of passage of the activation barrier is comparable to the relaxation time of the condensed medium (solvent). The population of the activated state gets depleted and one arrives at the friction-affected chemical kinetics described by the Kramers theory² and its modifications.³ For ET, this regime corresponds to solvent-controlled reactions when the preexponential factor of the rate is inversely proportional to a solvent relaxation time.⁴ One can anticipate the next step in this hierarchy of relaxation times when the time of the reaction itself (not just the time of barrier passage) becomes comparable to the solvent relaxation time. Such conditions, which apply to ultra-fast reactions in high-temperature solvents and to reactions in slowly-relaxing viscous solvents, will result in the loss of ergodicity of the system and the break-down of the equilibrium description of the

reaction activation barrier (in contrast to the alteration of the rate preexponent in the Kramers description).⁵ A general theory of chemical rates at such conditions is still missing even though nonergodic behavior may apply to a broad class of reactions in supercooled liquids and in biopolymers.⁶ The latter case is particularly relevant to the problem of nonergodic activation since the dynamics of biopolymers is characterized by a broad spectrum of relaxation times,^{7,8} and, for a given reaction rate, at least a subset of nuclear modes may become nonergodic.

As the second cumulant of the difference in the solute-solvent interaction potential (eq 1), the solvent reorganization energy of ET is related to a response function of the solvent to the presence of the solute. The latter can be related to the susceptibility of the pure solvent corresponding to a nuclear collective coordinate coupled to the solute electronic states (dipolar polarization and density for dipolar solvents, quadrupolar polarization and density for non-dipolar solvents).⁹ Susceptibilities, which are second derivatives of a thermodynamic potential, are known to show specific behavior at points of thermodynamic instability (phase transitions) or at the onset of nonergodicity (glass transition). It is of general interest to understand how chemical reactions are affected by these special points. For glass transitions, the heat capacity of a glassformer (the second cumulant of energy at constant volume or the second cumulant of entropy at constant pressure) passes through a peak which sharpens with increasing fragility of the liquid.¹⁰ In this Letter we present simulation results indicating that the solvent reorganization energy of ET demonstrates a similar behavior. It first increases with lowering temperature and then sharply drops at the temperature of kinetic glass transition.

II. SIMULATION RESULTS

We perform *NVE* and *NPT* molecular-dynamics (MD) simulations for a system composed of one solute (*p*-nitroaniline) and $N = 466$ water molecules, with periodic boundary conditions. The extended simple point charge

*E-mail: dmitrym@asu.edu.

model (SPC/E) is adopted for water. *p*-nitroaniline is a small charge-transfer dye with a charge-transfer electronic transition resulting in about 3.7 D change in the dipole moment.¹¹ Its interaction with water is a sum of Coulomb interactions between solute and solvent partial charges and Lennard-Jones (LJ) potentials for which Lorentz-Berthelot combination rules are used. The *NVE* simulations are done for a cubic simulation cell with the side length of 24.075 Å and water density of 0.997 gm/cm³. The cutoff radius of 12.0 Å was employed. Simulations have been carried out in the range of temperatures from supercooled region (50 K) to superheated region (509 K).^{12,13,14,15} In parallel to solvation simulations, simulations of the pure SPC/E water ($N = 466$) at the same thermodynamic conditions have been done. Equilibration has been carried out over a time period of 400 ps and production runs have been accumulated over the duration of 1.0 ns at 509 K up to 6.0 ns at 50 K from configurations stored at the interval of 0.1 ps.

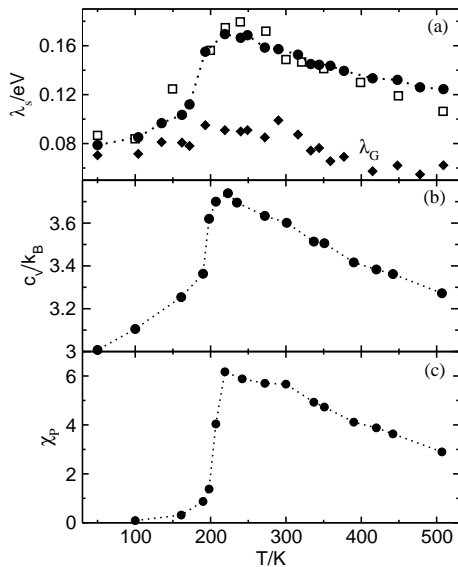


FIG. 1: Reorganization energy (a), heat capacity (b), and dielectric susceptibility (c) vs T . In (a), circles refer to *NVE* simulations at $\rho = 0.9997$ cm³/g, squares indicate the *NPT* simulations at $P = 1$ atm, diamonds refer to the fast Gaussian component of the solvent reorganization energy, λ_G . Dotted lines are drawn to guide the eye.

Atomic charges of *p*-nitroaniline were obtained by fitting the electrostatic potential from *ab initio* electron structure calculations using GAUSSIAN'03.¹⁶ The ground state geometry of *p*-nitroaniline was obtained on the MP2 level (6-31+G*) using X-ray data¹⁷ for the initial geometry. The excited-state charge distribution is obtained from SCI calculations. The ground, 7.18 D, and excited, 10.88 D, dipoles are in reasonable agreement with the literature data.^{11,18} Coordinates and charges of *p*-nitroaniline in the ground and excited states are listed in the supplement.

Figure 1(a) shows the solvent reorganization energy

calculated according to eq 1 in which the energy gap ΔE is replaced with the difference of the solute-solvent interaction potential in the charge-transfer (S_4) and ground (S_0) electronic states.¹¹ The average is performed over the simulation trajectories generated for the solute in the ground state. Circles indicate constant-volume simulations and squares refer to simulations at constant pressure of $P = 1$ atm. The reorganization energy increases with lowering temperature in the high-temperature liquid⁹ and then turns down and drops sharply at $T^* \simeq 219$ K.

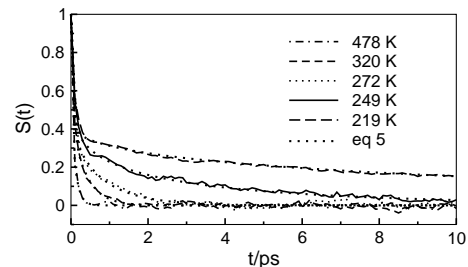


FIG. 2: Stokes shift correlation function (eq 4) of ground-state *p*-nitroaniline in SPC/E water.

Shown in Figure 1(b,c) are also the heat capacity,

$$c_V/k_B = 3/2 + \langle(\delta E)^2\rangle/N(k_B T)^2 \quad (2)$$

and dielectric susceptibility

$$\chi_P = (k_B T V)^{-1} \langle(\delta \mathbf{M})^2\rangle \quad (3)$$

of SPC/E water (E is the total energy and \mathbf{M} is the total dipole moment of a sample of liquid with volume V containing N molecules). Both solvent susceptibilities show the dependence on temperature very similar to that of λ_s . Figure 1 thus stresses the similarity in the temperature variation of the ET reorganization energy and susceptibilities of the pure solvent at the onset of nonergodicity at $T = T^*$.

The reorganization energy does not drop to zero, but instead levels off at low temperatures. The low-temperature component of λ_s is related to fast phonon-like solvent modes which do not become dynamically arrested below T^* . The fast reorganization component is clearly seen as the initial Gaussian decay of the Stokes shift correlation function¹⁹ (Figure 2)

$$S(t) = C(t)/C(0), \quad C(t) = \langle\Delta E(t)\Delta E(0)\rangle. \quad (4)$$

$S(t)$ was fitted to a biphasic form containing the Gaussian (G) and stretching exponential (E) parts

$$S(t) = A_G e^{-(t/\tau_G)^2} + (1 - A_G) e^{-(t/\tau_E)^\beta}. \quad (5)$$

The stretching exponent β obtained from the fit is equal to one above 272 K and starts to drop below this temperature reaching the value of 0.34 at 219 K (see the supplement).

From the fit of the simulated Stokes shift data, the Gaussian relaxation time¹⁹ $\tau_G \simeq 70$ fs is weakly temperature dependent and is approximately given by a linear function of T (K): $\ln(\tau_G(T)/\text{ps}) = -1.34 - 0.0042 \times T$ (Figure 3). In contrast, the exponential relaxation time τ_E increases sharply with lowering T and can be approximated by the Vogel-Fulcher (VF) law: $\ln(\tau_E(T)/\text{ps}) = -3.73 + 447/(T - 161)$, where T is in K.²⁰ The Gaussian reorganization component, $\lambda_G = A_G \lambda_s$, turns out to be weakly dependent on temperature (Figure 1(a), diamonds). The combination of the weak temperature dependence of λ_G with the ultra-fast relaxation of the Gaussian component of $S(t)$ clearly indicates that it is the slow exponential component of $S(t)$ that becomes dynamically arrested at the transition to nonergodicity. The drop of λ_s at $T < T^*$ is thus equal to $\lambda_E = (1 - A_G)\lambda_s$.

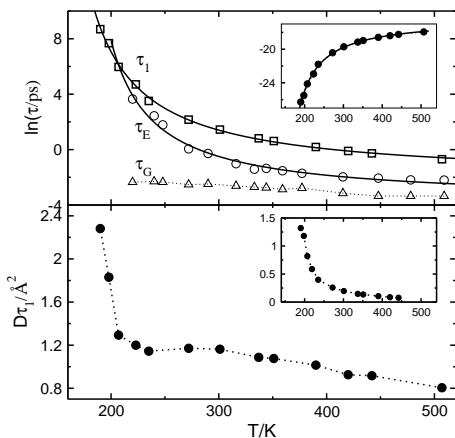


FIG. 3: Upper panel: Relaxation times τ_G , τ_E and τ_1 vs T . The inset shows natural logarithm of the diffusion coefficient D (m^2/s). The solid lines indicate the VF fits. Lower panel: The product of the self-diffusion coefficient and the rotational relaxation time τ_1 vs T . The inset shows the maximum value $\alpha_2(t^*)$ of the non-Gaussian parameter $\alpha_2(t)$ defined by eq 8.

The slow component of the Stokes shift dynamics can be identified with collective orientational relaxation of the dipolar polarization of water related to the frequency-dependent dielectric constant $\epsilon(\omega)$. The variation of $\epsilon(\omega)$ with lowering temperature is characteristic of many polar glassformers (Figure 4).²¹ In particular, the peak ω_{max} of the dielectric loss $\epsilon''(\omega)$ shifts to lower frequencies with cooling the solvent. The width of the dielectric spectrum, however, does not change, and the dielectric loss data at different temperatures can be superimposed on one master curve by proper re-scaling (Figure 4, upper panel). The increase in the width of dielectric loss is commonly associated with liquid heterogeneity.²¹ Figure 4 thus indicates that dielectric response is homogeneous.

The collective relaxation of solvation shells reflected by $\tau_E(T)$ can be compared to the single-particle correlation function of the dipole vector $\mathbf{m}(t)$:

$$C_1(t) = \langle \mathbf{m}(t) \cdot \mathbf{m}(0) \rangle / \langle \mathbf{m}(0)^2 \rangle. \quad (6)$$

The relaxation time $\tau_1(T)$ for $C_1(t)$ shows a super-Arrhenius temperature dependence similar to $\tau_E(T)$ (Figure 3) which can be approximated by the VF law: $\ln(\tau_1(T)/\text{ps}) = -2.15 + 578/(T - 137)$.

What is the nature of the dynamical arrest occurring below $\simeq 219$ K? Previous extensive simulations of SPC/E water have shown a power-law temperature dependence of transport coefficients with the critical temperature of ca. $T_c \simeq 186 - 200$ K.^{22,23,24,25} Based on this observation and scaling laws for the intermediate scattering function, the critical temperature was assigned to the ideal ergodic-to-nonergodic kinetic glass transition predicted by the mode-coupling theory (MCT).²⁶ Our data for the self-diffusion coefficient of SPC/E water $D(T)$ (obtained from MD trajectories using the Einstein relation) embrace a broader range of temperatures than those reported in refs 22 and 23. The self-diffusion coefficient (Figure 3, inset) can be fitted by both the power-law ($\ln(D(T) \times \text{s}/\text{m}^2) = -19 + 2.5 \ln(T/181 - 1)$) and VF ($\ln(D(T) \times \text{s}/\text{m}^2) = -16.5 + 540/(T - 136)$) functions, with the latter providing a better global fit. The limiting VF temperatures for single-particle correlations reflected by $D(T)$ and $C_1(T)$ (136 K and 137 K, respectively) are significantly lower than the corresponding temperature (161 K) from the many-particle correlation time $\tau_E(T)$.²⁰

The temperature T^* at which $\lambda_s(T)$ and solvent susceptibilities start to drop also marks the onset of the separation of translational and rotational diffusion signaling the breakdown of the Stokes-Einstein relation (Figure 3, lower panel)

$$D(T) \times \tau_1(T) \simeq \text{const} \quad (7)$$

Indeed, the product of the diffusion coefficient and the rotational relaxation time is approximately constant down to the temperature $T_c \simeq 207$ K.²⁷ If 165 K is adopted as the glass transition temperature for water,²⁰ the onset of translational enhancement falls in the range 1.2–1.3 T_g found in laboratory experiment.²⁸ This effect is commonly explained by either static spatial^{29,30,31,32} or dynamic³³ heterogeneity. In the frustration-limited domain picture of Tarjus and Kivelson,^{29,30} the turning temperatures in Figures 1 and 3 can be associated with the onset of domain formation. This interpretation is questionable, however, given the small size of our simulation box which cannot incorporate mesoscopic domains. Note also that no discontinuous change in pair distribution functions is observed at T^* except previously observed^{23,34} sharpening of solvation shell peaks.

The results of our simulations better fit the picture of spatially heterogeneous dynamics which assumes the presence in a supercooled liquid of groups of mobile molecules.^{33,35,36} These groups may represent clusters of hydrogen bond defects in SPC/E water,³⁶ chains of mobile particles in monoatomic LJ fluids,³⁵ or some other structures. The collective motion of such mobile heterogeneities provides the enhancement of translational diffusion which is correlated with the increase of the non-

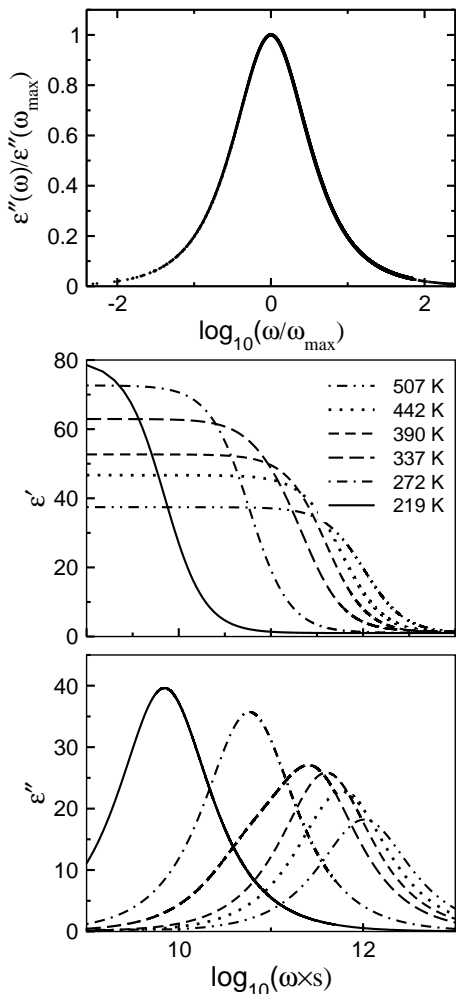


FIG. 4: Real ($\epsilon'(\omega)$) and imaginary ($\epsilon''(\omega)$) parts of the frequency-dependent dielectric constant of SPC/E water at different temperatures. The upper panel shows the re-scaled dielectric loss $\epsilon''(\omega)/\epsilon''(\omega_{\max})$ vs $\log_{10}(\omega/\omega_{\max})$ calculated at 198, 219, 242, and 300 K; ω_{\max} is the frequency maximum of the dielectric loss function. The data points at different temperatures cannot be distinguished on the plot scale.

Gaussian parameter³⁵

$$\alpha_2(t) = 3\langle r^4(t) \rangle / 5\langle r^2(t) \rangle^2 - 1, \quad (8)$$

where $\langle r^2(t) \rangle$ is the mean square displacement. The maximum value $\alpha_2(t^*)$ (Figure 3 lower panel inset) is reached at time t^* . Both $\alpha_2(t^*)$ and t^* grow with cooling indicating increasing dynamic heterogeneity of molecular trans-

lations. On the other hand, dielectric loss data show no heterogeneity suggesting a more homogeneous distribution of molecular rotations.

This interpretation is consistent with recent dielectric data by Richert *et al.*³⁷ which do not show any increase in spatial heterogeneity in the region of temperatures $T_g \leq T \leq 1.2T_g$ where previous reports³² had indicated the breakdown of the Stokes-Einstein relation. Although no broadly accepted explanation of this phenomenon currently exists, the onset of translation/rotation decoupling is normally associated with the critical MCT temperature. We will therefore resort to the interpretation of temperature T^* at which λ_s dips to its Gaussian component as the point of kinetic transition to nonergodicity with many features of the critical temperature of an ideal glass transition predicted by MCT.²⁶

III. CONCLUDING REMARKS

The MCT critical temperature T_c located above the calorimetric glass transition temperature marks the change in the mechanism of relaxation in viscous liquids. Above T_c , transport phenomena and response to a solute field are dominated by the rattling and librations of particles in self-consistently maintained cages. Below T_c , on the other hand, the particles are almost arrested in the free-energy landscape and transport and relaxation are triggered by thermally activated hopping and rotation over saddle points. The hopping mechanism is recorded by experiments with the observation window up to 10^2 s in the temperature range $T_g \leq T \leq T_c$. Many redox reaction occur on the nanosecond and faster time-scale. Since hopping relaxation does not occur on the reaction time-scale, MCT formalism may appear to be appropriate for describing ET reactions in viscous supercooled liquids. The sharp drop of the solvent reorganization energy close to T_c found in our simulations is therefore expected to mimic the laboratory ET experiment.

Acknowledgments

This research was supported by the National Science Foundation (CHE-0304694). This is publication #643 from the ASU Photosynthesis Center. Useful discussions with Prof. C. A. Angell and Prof. R. Richert are gratefully acknowledged.

¹ Marcus, R. A. *Rev. Mod. Phys.* **1993**, 65, 599.

² Gardiner, C. W. *Handbook of stochastic methods*; Springer: Berlin, 1997.

³ Grote, R. F.; Hynes, J. T. *J. Chem. Phys.* **1980**, 73, 2715.

⁴ Barzykin, A. V.; Frantsuzov, P. A.; Seki, K.; Tachiya, M.

Adv. Chem. Phys. **2002**, 123, 511.

⁵ Matyushov, D. V. *J. Chem. Phys.* **2005**, 122, 084507.

⁶ Dick, L. A.; Malfant, I.; Kuila, D.; Nebolsky, S.; Nock, J. M.; Hoffman, B. M.; Ratner, M. A. *J. Am. Chem. Soc.* **1998**, 120, 11401.

- ⁷ Frauenfelder, H.; Parak, F.; Young, R. D. *Ann. Rev. Biophys. Biophys. Chem.* **1998**, *17*, 451.
- ⁸ Andreatta, D.; Pérez, J. L.; Kovalenko, S. A.; Ernsting, N. P.; Murphy, C. J.; Coleman, R. S.; Berg, M. A. *J. Am. Chem. Soc.* **2005**, *127*, 7270.
- ⁹ Matyushov, D. V. *J. Chem. Phys.* **2004**, *120*, 7532.
- ¹⁰ Angell, C. A. *Science* **1995**, *267*, 1924.
- ¹¹ Farztdinov, V. M.; Schanz, R.; Kovalenko, S. A.; Ernsting, N. P. *J. Phys. Chem. A* **2000**, *104*, 11486.
- ¹² Stanley, H. E.; Buldyrev, S. V.; Canpolat, M.; Mishima, O.; Sadr-Lahijany, M. R.; Scala, A.; Starr, F. W. *Phys. Chem. Chem. Phys.* **2000**, *2*, 1551.
- ¹³ Debenedetti, P. G.; Stanley, H. E. *Phys. Today* **2003**, *56*, 40.
- ¹⁴ Vega, C.; Sanz, E.; Abascal, J. L. F. *J. Chem. Phys.* **2005**, *122*, 114507.
- ¹⁵ Giovambattista, N.; Angell, C. A.; Sciortino, F.; Stanley, H. E. *Phys. Rev. Lett.* **2004**, *93*, 047801.
- ¹⁶ Frisch, M. J.; Trucks, G. W.; Scuseria, G. E.; Robb, M. A.; Cheeseman, J. R.; Zakrzewski, V. G. *GAUSSIAN 03*; Pittsburgh, PA: 2003.
- ¹⁷ Donohue, J. *Acta Cryst.* **1956**, *9*, 960.
- ¹⁸ Rashid, A. N. *J. Mol. Struct.* **2004**, *681*, 57.
- ¹⁹ Jimenez, R.; Fleming, G. R.; Kumar, P. V.; Maroncelli, M. *Nature* **1994**, *369*, 471.
- ²⁰ The Vogel-Fulcher temperature for $\tau_E(T)$ falls slightly below $T_g \simeq 165$ K recently identified as the glass transition temperature of water, see Y.-Z. Yu and C. A. Angell, *Nature (London)* **2004**, *427*, 717.
- ²¹ Dixon, P. K.; Wu, L.; Nagel, S. R.; Williams, B. D.; Carini, J. P. *Phys. Rev. Lett.* **1990**, *65*, 1108.
- ²² Gallo, P.; Sciortino, F.; Tartaglia, P.; Chen, S.-H. *Phys. Rev. Lett.* **1996**, *76*, 2730.
- ²³ Sciortino, F.; Gallo, P.; Tartaglia, P.; Chen, S.-H. *Phys. Rev. E* **1996**, *54*, 6331.
- ²⁴ Fabbian, L.; Latz, A.; Schilling, R.; Sciortino, F.; Tartaglia, P.; Theis, C. *Phys. Rev. E* **1999**, *60*, 5768.
- ²⁵ Theis, C.; Sciortino, F.; Latz, A.; Schilling, R.; Tartaglia, P. *Phys. Rev. E* **2000**, *62*, 1856.
- ²⁶ Götze, W. Aspects of structural glass transitions. In *Liquids, freezing and glass transition*, Vol. 1; Hansen, J. P.; Levesque, D.; Zinn-Justin, J., Eds.; Elsevier: Amsterdam, 1991.
- ²⁷ The temperature $T_c = 207$ K from the plot of $D(T)\tau_1(T)$ vs T is very close to the estimate for the critical temperature $T_c \simeq 208$ K from the molecular MCT with a restricted set of correlation functions (dipole approximation).²⁴ This agreement is, however, fortuitous since the full version of the molecular MCT leads to a substantially higher temperature, $T_c \simeq 279$ K.²⁵
- ²⁸ Chang, I.; Sillescu, H. *J. Phys. Chem. B* **1997**, *101*, 8794.
- ²⁹ Tarjus, G.; Kivelson, D. *J. Chem. Phys.* **1995**, *103*, 3071.
- ³⁰ Kivelson, D.; Tarjus, G. *Phil Mag. B* **1998**, *77*, 245.
- ³¹ Xia, X.; Wolynes, P. G. *J. Phys. Chem. B* **2001**, *105*, 6570.
- ³² Swallen, S. F.; Bonvallet, P. A.; McMahon, R. J.; Ediger, M. D. *Phys. Rev. Lett.* **2003**, *90*, 015901.
- ³³ Jung, Y. J.; Garrahan, J. P.; Chandler, D. *Phys. Rev. E* **2004**, *69*, 061205.
- ³⁴ Donati, C.; Glotzer, S. C.; Poole, P. H.; Kob, W.; Plimpton, S. J. *Phys. Rev. E* **1999**, *60*, 3107.
- ³⁵ Schober, H. R. *Phys. Chem. Chem. Phys.* **2004**, *6*, 3654.
- ³⁶ Giovambattista, N.; Mazza, M. G.; Buldyrev, S. V.; Starr, F. W.; Stanley, H. E. *J. Phys. Chem. B* **2004**, *108*, 6655.
- ³⁷ Richert, R.; Duvvuri, K.; Duong, L.-T. *J. Chem. Phys.* **2003**, *118*, 1828.